Available online at www.sciencedirect.com
ScienceDirect
Thermochimica Acta 459 (2007) 94–103
thermochimica acta
www.elsevier.com/locate/tca

Kinetic and thermodynamic studies of the formation of a polyurethane based on 1,6-hexamethylene diisocyanate and poly(carbonate-*co*-ester)diol

B. Fernandez d'Arlas [a], L. Rueda [a], P.M. Stefani [b], K. de la Caba [a], I. Mondragon [a], A. Eceiza [a,*]

[a] *"Materials+Technologies" Group, Department of Chemical and Environmental Engineering, Eskola Politeknikoa/Escuela Politécnica, Euskal Herriko Unibertsitatea, Pza. Europa 1, 20018 Donostia-San Sebastián, Spain*

[b] *Research Institute of Material Science and Technology (INTEMA), Engineering Faculty, Mar del Plata University, Juan B. Justo 4302, 7600 Mar del Plata, Argentina*

Received 6 February 2007; received in revised form 26 March 2007; accepted 31 March 2007
Available online 5 April 2007

Abstract

This paper presents the kinetic and thermodynamic characterization of a non-catalyzed reaction between poly(hexamethylene carbonate-*co*-caprolactone)diol (PHMC-*co*-PCL) and aliphatic hexamethylene diisocyanate (HDI) with a stochiometric functional concentration, using both isothermal and dynamic differential scanning calorimetry, DSC, as well as Fourier transform infrared spectroscopy, FT-IR. DSC data were fitted using a Kamal autocatalytic equation. Model-free-isoconversional methods were also applied to analyse the conversion dependence of the global activation energy. This relation was used to predict the reaction conversion versus time pattern at different temperatures and to compare it with that of the model approach. Kinetic modelling and model-free analysis successfully described the conversion versus time curves. The reaction can be divided in two different paths: the forward path and the autocatalyzed one. Results corroborated that autocatalysis is promoted by the urethane group. Activation energies for both reaction paths have been found to be higher than those presented in the literature for aromatic diisocyanate systems, which explains the lower reaction rate of the presented system.

Keywords: Aliphatic polyurethane; Kinetics; Autocatalysis; Kamal; Model-free-isoconversional

1. Introduction

Polyurethanes are very versatile polymers which allow creating new promising materials. This is mainly due to the way they are synthesized and the wide range of different components that can be used to form diverse polyurethanes. Segmented thermoplastic polyurethane elastomers (STPUEs) based on poly(ester)urethanes and poly(carbonate)urethanes have been claimed to be promising biodegradable materials with potential utilities in biomedical sciences applications, as long term medical implants, mainly in blood contact devices [1–6]. These polyurethanes have received great attention as they posses a broad range of chemical and physical properties, good biocompatibility and can be designed to degrade in biological environments due to the possibility of easily varying their chemical composition. In previous work, commercially synthesized polyurethanes were prepared with no completely biocompatible precursors [1,5,6]. In this work, hexamethylene diisocyanate, which is claimed as not toxic amine producer during degradation of the corresponding polyurethanes [1,6], has been used. No catalyst was employed for avoiding biocompatibility problems of the material.

Knowledge of kinetic parameters of a reactive resin is essential on the design and processing of polymer and composite technologies. Kinetic prediction of the cure pattern over a wide temperature range is also of interest. The present polyurethane addition reaction was followed by Fourier transform infrared spectroscopy (FT-IR) and by differential scanning calorimetry

* Corresponding author.
E-mail address: arantxa.eceiza@ehu.es (A. Eceiza).

0040-6031/$ – see front matter © 2007 Elsevier B.V. All rights reserved.
doi:10.1016/j.tca.2007.03.021

(DSC) at several isothermal temperatures and also dynamically by means of DSC. In this work an autocatalytic kinetic model and model-free-isoconversional methods were applied for the characterization of the reaction of the chosen polyurethane system and to compare the applicability of the methods to the present aliphatic elastomeric polyurethane cure.

2. Background

2.1. Kinetic modelling

Kinetic models developed from kinetic analysis of DSC data have been widely applied to epoxy-thermosetting resins cure [7–13]. Some authors have recently presented their application to the study of polyurethanes cure [14–19]. These methods have also been applied to kinetic studies of solid to solid and gas transitions [20], unsaturated polyesters cure [21–23], allotropic transitions [24], cure of benzoxazine resins [25], cure of phenolic resins [26], or diffusion controlled reaction kinetics [27], among others.

In the simplest way, using the definition of conversion, for polyurethane addition reaction, $\alpha = 1 - [\mathrm{NCO}]_t/[\mathrm{NCO}]_0$, with $[\mathrm{NCO}]_t$ and $[\mathrm{NCO}]_0$ being the isocyanate concentration at any reaction time and at the beginning, respectively, reaction rate can be described by the general equation:

$$\frac{\mathrm{d}\alpha}{\mathrm{d}t} = k(T)f(\alpha) \tag{1}$$

where $\mathrm{d}\alpha/\mathrm{d}t$ is the reaction rate, $k(T)$ is a constant depending only on temperature and $f(\alpha)$ an unknown function of conversion.

$k(T)$ is usually represented by Arrhenius relationship:

$$k = A\exp\left[\frac{-E_\mathrm{a}}{RT}\right] \tag{2}$$

where E_a is the activation energy of the reaction, T the absolute temperature, R the universal gas constant, and A is the preexponential or frequency factor, which gives an idea of the association tendency of reacting molecules. As Eqs. (1) and (2) show, the higher the frequency factor is, the faster the reaction.

In Eq. (1), $f(\alpha)$ is chosen according to experimental data and describes the reaction mechanism. There are many different proposed functions for the function $f(\alpha)$. Some of them are compared in Ref. [12]. One common reaction function is that of nth order:

$$f(\alpha) = (1-\alpha)^n \tag{3}$$

Substitution of Eqs. (3) into (1) yields an equation representing a mechanism with maximum reaction rate at $\alpha = 0$, that is at the beginning of the reaction.

Another function is the so-called Prout–Tompkins equation [28]:

$$f(\alpha) = \alpha^m(1-\alpha)^n \tag{4}$$

Eq. (4) describes an autocatalytic process with initial reaction rate equal to zero.

The generalization of mechanisms described by combination of Eqs. (3) and (4) into (1) is the so-called Kamal–Sourour [21] autocatalytic equation:

$$\frac{\mathrm{d}\alpha}{\mathrm{d}t} = (k_1 + k_2\alpha^m)(1-\alpha)^n \tag{5}$$

where n, m, reaction orders, and k_1, k_2, kinetic constants, can be obtained using Kenny proposed iterative method [29] by means of DSC isothermal data.

A commonly accepted mechanistic equation to describe some polyurethanes non-catalyzed alcohol, –OH, and isocyanate, –NCO, reaction rate is the so-called Sato's equation [30]:

$$-\frac{\mathrm{d}[\mathrm{NCO}]}{\mathrm{d}t} = K_1[\mathrm{NCO}][\mathrm{OH}]^2 + K_2[\mathrm{NCO}][\mathrm{OH}][\mathrm{RNHCOOR}\prime] \tag{6}$$

which gives account of an alcohol and urethane, –RNHCOOR′–, autocatalyzed mechanism. Taking into account the definition of conversion, this equation can be rewritten in the following form [31]:

$$\frac{\mathrm{d}\alpha}{\mathrm{d}t} = (k_1 + k_2\alpha)(1-\alpha)^2 \tag{7}$$

being $k_1 = K_1/A_0^2$ and $k_2 = (K_2 - K_1)A_0^2$ the absolute rate constants and $A_0^2 = [\mathrm{NCO}]_0^2 = [\mathrm{OH}]_0^2$.

In order to compare our system kinetics pattern with that found in the literature, different modelling methods have been applied.

2.2. Model-free-isoconversional methods

The advantage of analysing kinetic data using model-free methods is that they do not assume any model or mechanism beforehand, and thus they are able to predict the most complicated reaction behaviour even at a different range of temperatures. Vyazovkin and coworkers [7–9] have deeply developed these methods, and good critical reviews are also available [32–34].

The main assumption of these methods is that the reaction mechanism does not change with temperature and heating rate. The principle of isoconversional methods is that theoretically the kinetic constants, at a determined conversion, are only function of the temperature.

Isoconversional methods do not provide mechanism details. They describe the kinetics with an average activation energy function of conversion and temperature [32]. Thereby they assume that the reaction rate can be expressed as a product of a function of the temperature and a function of the conversion similar to Eq. (1).

2.2.1. Isoconversional–isothermal methods

These require curing under isothermal conditions at different temperatures.

2.2.1.1. Integral method. Assuming that $k(T)$ has an Arrhenius temperature dependence, this method uses integral form of Eq.

(1) over a range $\langle 0, \alpha \rangle$:

$$g(\alpha) = \int_0^{\alpha} \frac{d\alpha}{f(\alpha)} = A t_\alpha \exp\left[\frac{-E_a}{RT}\right] \quad (8)$$

where $g(\alpha)$ is an unknown function of the conversion and t_α is the time required to reach a conversion α at a temperature T. Taking logarithms from Eq. (8):

$$\ln(t_\alpha) = \ln\frac{g(\alpha)}{A} + \frac{E_a}{RT} \quad (9)$$

For a constant conversion, a plot of $\ln(t_\alpha)$ versus $1/T$ should lead to a straight line whose slope allows the calculation of the activation energy for that given conversion. From the origin intercept the value for $g(\alpha)/A$ at each conversion, assumed independent of the temperature, can be obtained. Using the integrated form of Eq. (8), the pair for each conversion $[E_a, g(\alpha)/A]_\alpha$ allows to predict the time required to reach that conversion at any other temperature.

As reported by many authors [32,33], this method is an approximation for considering a non-conversion dependent E_a when integrating Eq. (8). Vyazovkin has proposed a method [35] to solve this problem, using a numerical procedure for integration (8), in which the activation energy is not averaged over the integration range.

2.2.1.2. Differential or Friedman method [36]. This method is based on the logarithmic form of Eq. (1):

$$\ln\frac{d\alpha}{dt} = \ln A\, f(\alpha) - \frac{E_a}{RT} \quad (10)$$

For a constant value of α, a plot of $\ln(d\alpha/dt)$ versus $1/T$ should be a straight line whose slope allows the evaluation of E_a.

2.2.2. Isoconversional–dynamic methods

These methods require measurements of cure at different heating rates.

2.2.2.1. Differential or Friedman method. For non-isothermal conditions the reaction rate can be expressed as

$$\beta\frac{d\alpha}{dT} = A f(\alpha) \exp\left[\frac{-E_a}{RT}\right] \quad (11)$$

where β stands for the experiment heating rate and T is the absolute temperature.

From which, taking logarithms:

$$\ln \beta_i \frac{d\alpha}{dT} = \ln A f(\alpha) - \frac{E_a}{RT_\alpha} \quad (12)$$

where T_α is the temperature at which the system approach a conversion α, and β_i is a determined heating rate. For a constant α, a plot of $\ln \beta_i(d\alpha/dT)$ versus $1/T_\alpha$ should be a straight line whose slope allows the calculation of activation energy.

2.2.2.2. Integral methods. Those methods are based on the integration of Eq. (11):

$$g(\alpha) = \frac{A}{\beta}\int_0^{T} \exp\left[\frac{-E_a}{RT}\right] dT = \frac{AE}{\beta R}\, p(x) \quad (13)$$

where $x = E_a/RT$ and $p(x)$ is the so-called temperature or exponential integral which cannot be exactly calculated [32–35]. Actually, integral methods differ depending on the approximation of this integral. One of them is that given by Flynn and Wall [37], and Ozawa [38], which relies on Doyle approximation [39]:

$$\ln p(x) = -5.331 - 1.052x \quad (14)$$

Taking logarithms in (13) and substituting in (14):

$$\ln \beta = \ln\frac{AE}{Rg(\alpha)} - 5.331 - 1.052\frac{E_a}{RT} \quad (15)$$

For a constant conversion, a plot of $\ln \beta$ versus $1/T$, from the data at different heating rates, leads to a straight line whose slope provides E_a calculation. This method is known as Flynn–Wall–Ozawa method (FWO).

In the Kissinger–Akahira–Sunose method (KAS), the expression $p(x)$ is expressed using the Coats–Redfern approximation [40]:

$$p(x) \cong \frac{\exp[-x]}{x^2} \quad (16)$$

Substituting this into (13) and taking logarithms:

$$\ln\left(\frac{\beta}{T^2}\right) \cong \ln\left(\frac{AR}{g(\alpha)E_a}\right) - \frac{E_a}{RT} \quad (17)$$

A plot of $\ln(\beta/T^2)$ versus $1/T$ for a constant conversion gives the E_a at that conversion.

In this work both isothermal and non-isothermal presented methods have been applied.

3. Experimental

1,6-Hexamethylene diisocyanate (HDI) provided by Bayer (Desmodur® W) was used as received. This reactant was carefully manipulated as it has a low vapour pressure being potentially toxic by inhalation. The polydiol was poly(hexamethylene carbonate-*co*-caprolactone) (PHMC-*co*-PCL). This polymer was provided by Polimeri Europe, Ravena, with the commercial name of Ravecarb R111. It was dried under vacuum before use. The polydiol number-average-molecular weight is 2023 g/mol, as determined using ASTM-D 4274-88 standard for measuring the hydroxyl number. The block copolymer is formed by 45 wt% polycarbonate and 55 wt% polycaprolactone.

Sandwiches of KBr were prepared as sample containers for FT-IR measurements. The equipment used was a Nicolet-Nexus-FT-IR spectrometer provided with a temperature chamber and controller from Specac. Spectra of the samples were obtained averaging 20 scans between 4000 and 400 cm^{-1} with a resolution of 2 cm^{-1}.

To relate conversion with absorbance changes the area of isocyanate group, –N=C=O stretching band appearing at around 2273 cm^{-1}, A_{NCO}, was measured at different times and normalized with the area of a reference peak, in this case the C–H symmetric and antisymmetric stretching band spanning from 2950 to 2850 cm^{-1} approximately, A_{ref}, which does not significantly change during reaction [41]. Lambert–Beer law was assumed. Relative changes in molar absorbtivity for the isocyanate and for the reference band during the reaction were considered to be equal.

Isocyanate conversion was calculated as follows:

$$\alpha = 1 - \frac{(A_{NCO}/A_{ref})_t}{(A_{NCO}/A_{ref})_{t=0}} \quad (18)$$

Measurements were performed at 90, 110, 120, 130 and 140 °C.

Both isothermal and dynamic DSC scans were performed using a Mettler Toledo DSC822^e provided with a robotic-arm and with an intracooler. Isothermal runs were performed at temperatures ranging from 90 to 140 °C. Non-isothermal scans were undertaken at 5, 10, 15, 20, 30 and 40 °C/min heating rates and the range was from 30 to 200 °C. Material weighed for each reactive sample was in the range of 5–10 mg. All the runs were performed under inert N_2 atmosphere.

In the isothermal analysis conversion was calculated supposing a proportional ratio between heat flow and reaction rate. Then the conversion at each time was calculated referring the heat evolved until that moment, ΔH_t, to the total heat, the sum of the isothermal run heat plus the residual heat:

$$\alpha = 1 - \frac{\Delta H_t}{\Delta H_{iso} + \Delta H_{res}} \quad (19)$$

where ΔH_{iso} is the heat released during the isothermal measurement and ΔH_{res} is the residual heat measured dynamically after each isothermal cure at a heating rate of 30 °C/min from 30 to 200 °C. Very low residual heats were obtained in all cases, thus indicating that high conversions were reached during the isothermal measurements.

High resolution NMR spectra of the reaction reactants and products were recorded using a Bruker 300 MHz spectrometer. Samples were dissolved to 10 wt% in deuterated chloroform ($CDCl_3$). ^{13}C NMR chemical shifts were measured with respect to tetramethylsilane (TMS) as internal standard.

The following conditions were used: sweep width 18,832 Hz, pulse width = 5.5 μs, pulse delay = 10 s, acquisition time = 1.75 s, and data points = 65,500.

4. Results and discussion

4.1. Kinetic modelling

The mechanism and kinetics of uncatalyzed reactions of isocyanates with alcohols have been widely investigated [15,31,42–47]. Although the reaction is approximately of second order, it has been demonstrated that more complex equations are necessary. In the literature the autocatalytic effect has been attributed to alcohol and/or urethane catalysis, or to the consumption of NCO by side reactions as the formation of allophanates [47]. Side reactions have been checked by ^{13}C NMR, comparing spectra of both the polydiol and the formed polyurethane. Since urethane formation reaction from alcohol and isocyanate implies the disappearance of hydroxyl group and the formation of a new group, the urethane group, only carbonyl and alkyl groups bonded to polydiol hydroxyl and urethane groups were analysed. Fig. 1a presents the carbonyl region of ^{13}C NMR spectra of the raw polydiol, and that of stoichiometric polyurethanes cured at 120 and 140 °C. Fig. 1b corresponds

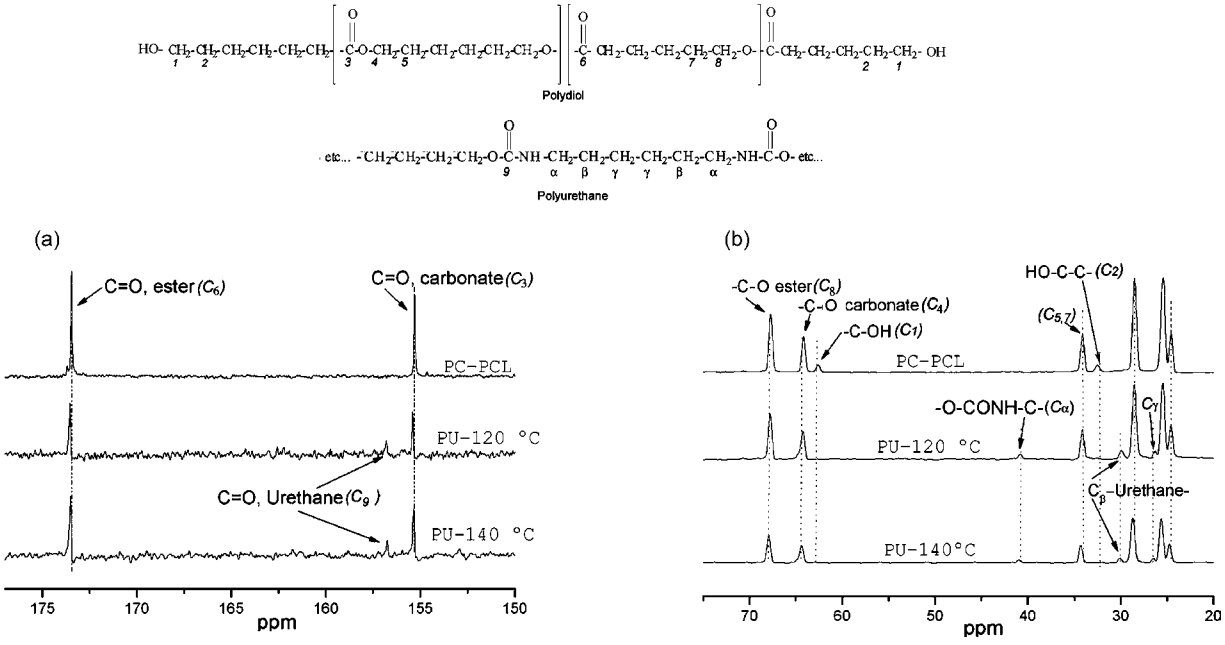

Fig. 1. ^{13}C NMR spectra for the raw polyol (PC-PCL) and stoichiometric polyurethanes cured at 140 °C (PU-140 °C) and 120 °C (PU-120 °C): (a) carbonyl region; (b) aliphatic carbons region.

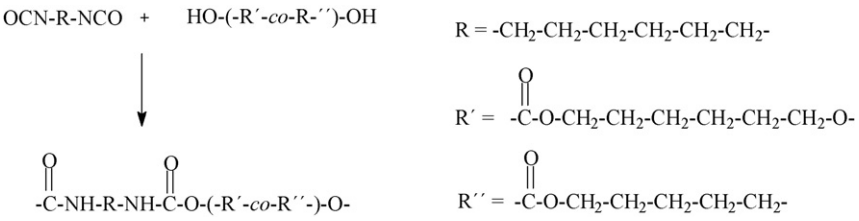

Scheme 1. Reaction studied and reactants formulas.

to the region of aliphatic carbons. The main difference between the reaction products and reactants is the disappearance of alkyl carbon, C_1, bonded to hydroxyl group band at 64 ppm, and alkyl carbon, C_2, bonded to hydroxyl bonded alkyl carbon band at 33 ppm, the formation of urethane carbonyl carbon, C_9, band at 156 ppm, alkyl carbon, C_α, band bonded to urethane nitrogen belonging to HDI monomer at 41 ppm, and alkyl carbon, C_β, band of HDI monomer bonded to alkyl carbon bonded urethane nitrogen at 30 ppm. Another alkyl carbon and attributed to HDI monomer, C_γ, can be seen at 26 ppm. Therefore, no substantial lateral reactions, such as those of isocyanurate or allophanate formation, were undergone within the temperature range studied, and only urethane linkages were obtained. Then the addition reaction between polydiol hydroxyl groups and isocyanate groups of HDI molecule to form urethane can be sketched as shown in Scheme 1.

A set of FT-IR spectra between 3100 and 1600 cm^{-1} obtained at 120 °C at different times is shown in Fig. 2. The disappearance of isocyanate antisymmetric stretching band at 2273 cm^{-1} through time as a consequence of the reaction between hydroxyl and isocyanate groups can be clearly seen. In the FT-IR spectra obtained at different temperatures within the range 4000–400 cm^{-1} no bands attributable to allophanate or isocyanurate formation were seen, thus being in accordance with ^{13}C NMR analysis results.

Fig. 3 shows the isothermal DSC thermograms obtained at different curing temperatures. As temperature increases the thermogram peak shifts toward shorter times being the whole process finished in less time. Infrared conversion obtained according to Eq. (18) and DSC conversion data obtained by Eq. (19) at different temperatures are shown in Fig. 4. This

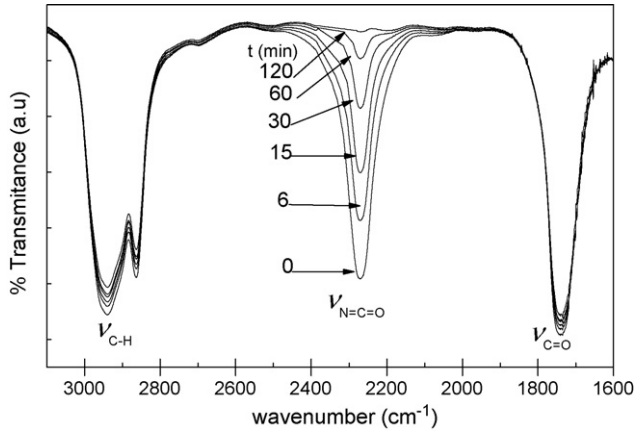

Fig. 2. FT-IR spectra of the reactive sample recorded at different times at 120 °C.

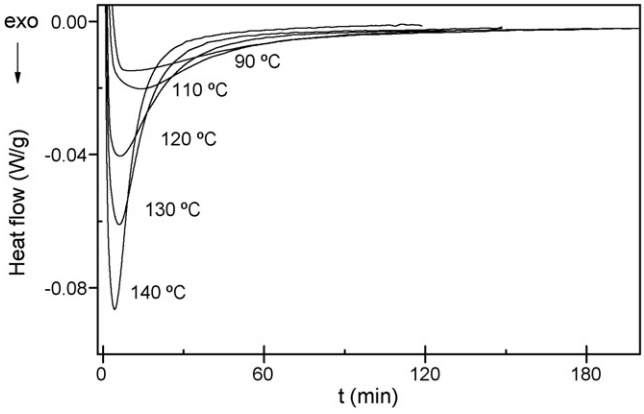

Fig. 3. Differential scanning calorimetry (DSC) isothermal thermograms of the reactive system at different temperatures.

shows the correlation of both methods on the measurement of the conversion for a given time. The relation $\alpha(t,T)$ was therefore considered the same for both techniques, and only DSC data were used for the following analysis. Moreover, the shift factor study gave a fairly neat superposition of α versus $\ln t$ curves at different temperatures as also presented in the right-hand side small square of Fig. 4. This fact can be attributed to reactions following the same mechanism within the range studied [18].

Fig. 5 shows the evolution of reaction rate with reaction conversion at different temperatures. As seen, the system presents an initial reaction rate different from zero and from the maximum. Therefore, the common nth order model cannot represent this system. Thus, $f(\alpha)$ function corresponding to Eqs. (3) and (4) was rejected for describing the present system.

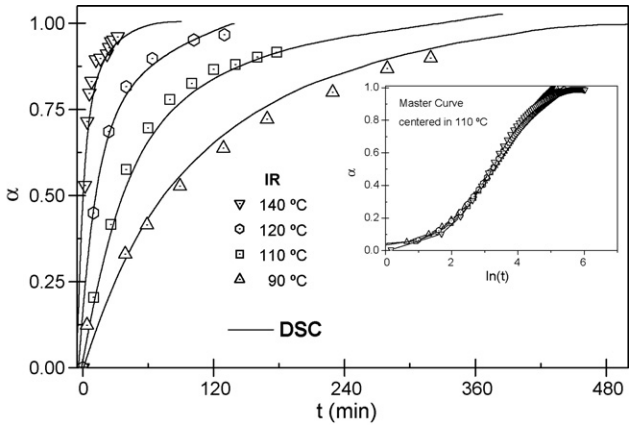

Fig. 4. Conversion vs. time for DSC and FT-IR measurements at different temperatures. The right-hand side small square represents the master curve, conversion vs. ln(t) centred at 110 °C.

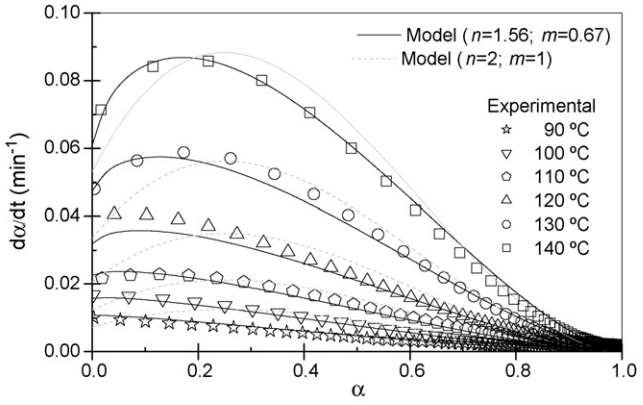

Fig. 5. Comparison of experiment results (symbols), with a model with $n = 2$ and $m = 1$ (dash line), and with the model obtained by iteration, with $n = 1.56$ and $m = 0.67$ (solid line).

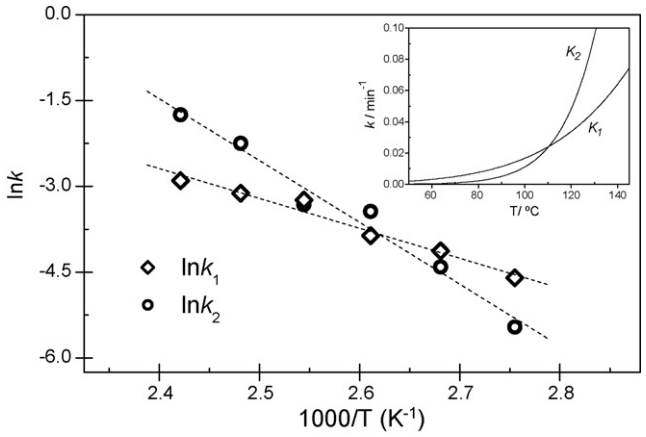

Fig. 6. Arrhenius plot for the Kamal model constants, calculated using Kenny's method. In the upper right corner square the constants are plotted against the temperature.

Previous studies [30,31,43–46] on polyurethane kinetics were able to describe the mechanism of non-catalyzed polyurethane formation and fit experimental data to a Kamal-shape autocatalytic equation with orders $n = 2$ and $m = 1$, represented by Eqs. (6) and (7). That case applied to polyurethanes fits the so-called Sato's autocatalytic equation [30]. DSC experimental data have been used in Eq. (7) to obtain k_1 and k_2 absolute kinetic parameters, via Runge–Kutta iteration, but as shown in Fig. 5 the model did not fit the experimental results. Although Sato's autocatalytic equation has been previously used to describe equimolecular aliphatic [48] and aromatic [43] diisocyanate/alcohol autocatalytic systems, that model was not able to describe the present autocatalytic polyurethane cure in the temperature range employed, slightly higher than those of most kinetic studies found in literature. Therefore, any reaction order was assumed using Kenny's iterative method [29]. When applying this method it was assumed $d\alpha/dt = k_1$ when $\alpha = 0$. At shown in Fig. 5, the DSC experimental data obtained at different temperatures fits well to Kamal–Sourour generalized autocatalytic Eq. (5) with $n = 1.56$ and $m = 0.67$ values for the range of temperature studied. According to these results, the global reaction rate of our system approaches the value $m + n = 2$ shown in the literature [19,29] for other systems.

The absolute k_1 and k_2 obtained values at each temperature are listed in Table 1. k_1/k_2 varied from 2.15 to 0.34 when increasing the temperature from 90 to 140 °C and $k_2 > k_1$ at temperatures above 110 °C, thus the autocatalytic effect becomes more noticeable at higher temperatures. Moreover, a m value lower than unity means that the autocatalytic reaction has higher contribution on the overall reaction rate.

Fig. 6 shows the Arrhenius plot for the obtained absolute constants using this method. Assuming Arrhenius-temperature-dependence, activation energies for both processes described by Eq. (5) were calculated from the slope of $\ln k$ versus $1/T$. The obtained parameters of this model are gathered in Table 1.

Isothermal experimental behaviour was compared to that predicted by the model with $n = 1.56$ and $m = 0.67$. For this purpose the model differential equations were integrated numerically to give time values at different conversions. Enough points were calculated in order to draw a neat curve. To draw each temperature isotherms by this method, kinetic constants k_1 and k_2 obtained by Kenny's iteration were used. These curves are presented in Fig. 7 together with DSC experimental isotherms. As seen the fitting is fairly neat within the whole range of conversion.

Frequency factors for non-catalyzed, A_1, and autocatalyzed, A_2, reaction pathways are also presented in Table 1. As seen frequency factors are $A_1 < A_2 < 10^{14}\ \text{min}^{-1}$, which is in accordance with general theory of reaction rates, since polymerization is a process in which the entropy diminishes during reaction [49].

Although frequency factors data ($A_2 \gg A_1$) indicate that associations of reactive molecules with urethane are more probable (i.e. A_2 higher), the higher activation energy obtained for autocatalysis hindrances this reaction path to occur before the non-catalyzed one. When increasing the temperature the

Table 1
General kinetic parameters of the autocatalytic Kamal model

T (°C)	$n = 1.56$			$m = 0.67$		
	k_1 ($\times 10_2$ min^{-1})	E_{a1} (kJ/mol)	A_1 (min^{-1})	k_2 ($\times 10^2$ min^{-1})	E_{a2} (kJ/mol)	A_2 (min^{-1})
90	1.05			0.50		
100	1.58			1.11		
110	2.26	43.5 ± 1.5	1.9×10^4	2.37	90.0 ± 2.5	4.2×10^{10}
120	3.26			4.85		
130	4.40			9.53		
140	6.03			18.38		

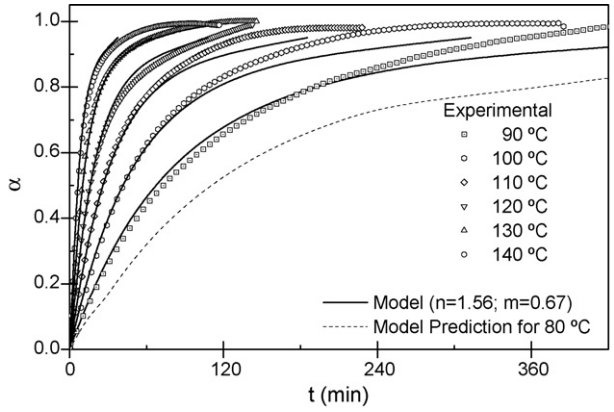

Fig. 7. Isothermal prediction of the autocatalytical model with $n = 1.56$ and $m = 0.67$, and raw isothermal data.

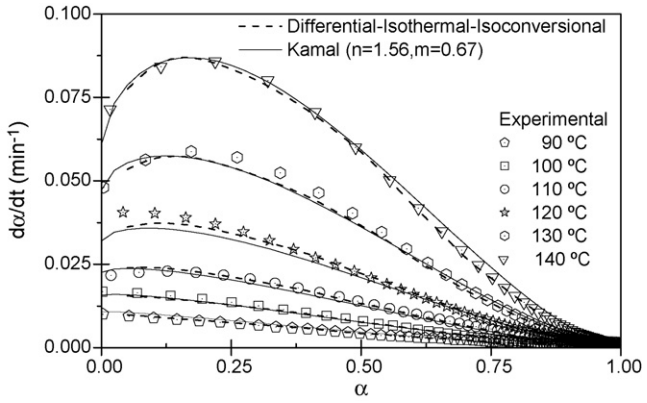

Fig. 9. Comparative of Kamal-autocatalytic fit with free-model-isothermal differential method and experimental results.

enthalpic effect to the reaction rate becomes flattered and the tendency to association, represented by the preexponential factor, gets more important, thus being the autocatalyzed reaction more important at higher temperatures. This is also explained below taking into account a thermodynamical consideration.

The activation energy values obtained in the present work are higher than the values reported in the literature for systems based on aromatic diisocyanates and polyols with similar molecular weigh [43], what gives account of the lower reactivity of aliphatic diisocyanates. In any case, the activation energy values obtained for urethane catalyzed pathway are the highest. These results then also follow the tendency appointed by other authors ($k_{aromatic} > k_{aliphatic}$, $E_{aromatic} < E_{aliphatic}$, and $E_2 > E_1$) [43–47].

4.2. Model-free-isoconversional-methods

4.2.1. Isothermal methods

Integral and Friedman differential isothermal methods were used to calculate the activation energies at different conversions. They were also analysed and used to draw the corresponding α versus t and $d\alpha/dt$ versus t, respectively. Fig. 8 presents Friedman plots of $\ln(d\alpha/dt)$ versus $1/T$ for different conversions. Activation energies calculated from the slopes were matched to the determined conversion. Friedman method was used as follows. First the pairs $A_\alpha = A\,f(\alpha)$, $B_\alpha = E_a/R$ were calculated for each conversion. The required plot is presented in Fig. 8. Then, those values were used to draw the reaction rate curves for each temperature using the non-logarithmic form of Eq. (10).

The resulting curves are shown together with the experimental data and with the Kamal obtained model using Kenny iterative method in Fig. 9.

The procedure used to draw the conversion versus time cure patterns by the integral method was utilized in the following way. First, the pairs $A_\alpha = A/g(\alpha)$, $B(\alpha) = E_a(\alpha)/R$, were calculated for different conversions, and then introduced into the integrated form of Eq. (8) for the calculation of time t_α required to reach a conversion α, at different temperatures T.

As mentioned above this method has the pitfall [32–35] of considering E_a an average between $\langle 0, \alpha \rangle$, for the integration in Eq. (8). Nevertheless, it gives errors less than 4% for the present system when drawing α versus t curves, as seen in Fig. 10. Integral method was used to predict the conversion versus time curve at 80 °C, which it is also gathered in Fig. 10.

As inferred from the fittings, we can say that both autocatalytic and model-free-isothermal models can be used to describe the whole reaction pattern of our system.

Activation energies as function of conversion calculated by Friedman and Integral isothermal methods are presented in

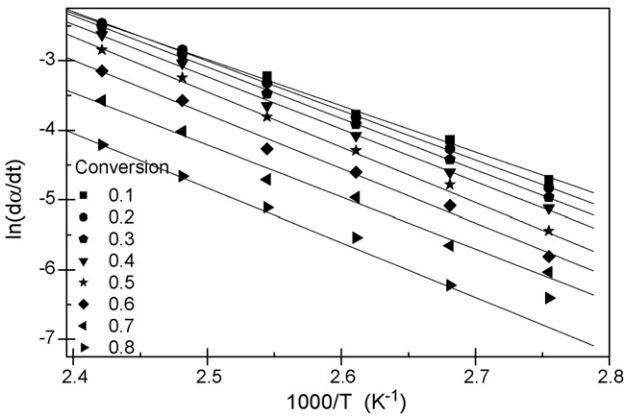

Fig. 8. Friedman plot for calculation of global reaction activation energy at different conversions.

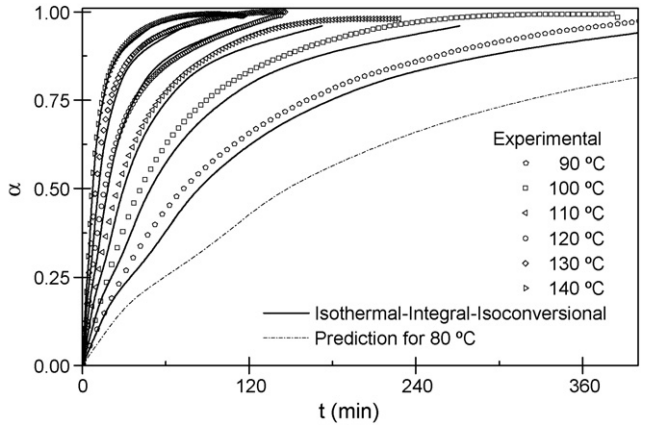

Fig. 10. Integral–isothermal–isoconversional method used to predict α vs. t curves.

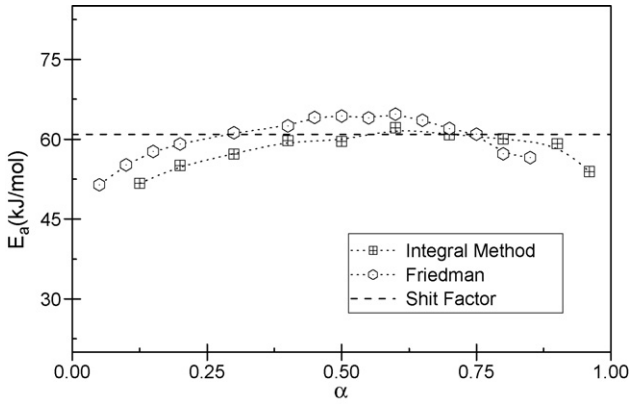

Fig. 11. Activation energies as function of conversion measured by different isothermal techniques.

Fig. 11. They are compared with the activation energy value calculated from the slope resulting by plotting the shift factors obtained from displacements of α versus $\ln(t)$ against $1/T$, which gives an average activation energy representative of the whole process. The convex pattern of $E(\alpha)$ values versus α shown in Fig. 11 are representative of an autocatalytic process with diffusion regime in its later stages [8].

4.2.2. Non-isothermal methods

Non-isothermal cures at different heating rates were also performed. The aim of this was to predict the isothermal cure. To obtain the $E(\alpha)$ dependence, Friedman, Flynn–Wall–Ozawa and Kissinger–Akahira–Sunose methods were applied. The resulted patterns are shown in Fig. 12. To predict the isothermal $\alpha(t)$ relationship upon non-isothermal data, the isoconversional relation proposed by Vyazovkin and coworkers [8,50] was used. According to this method, for a given conversion, the integral $g(\alpha)$, previously defined in Eqs. (8) and (13), must be equal for both isothermal experiments and non-isothermal methods.

Resolving (8) and (13) simultaneously:

$$g(\alpha) = \int_0^{\alpha} \frac{d\alpha}{f(\alpha)} = A t_\alpha \exp\left[\frac{-E_a}{RT_0}\right] = \frac{A}{\beta}\int_0^{T_\alpha} \exp\left[\frac{-E_a}{RT_\alpha}\right] dT \quad (20)$$

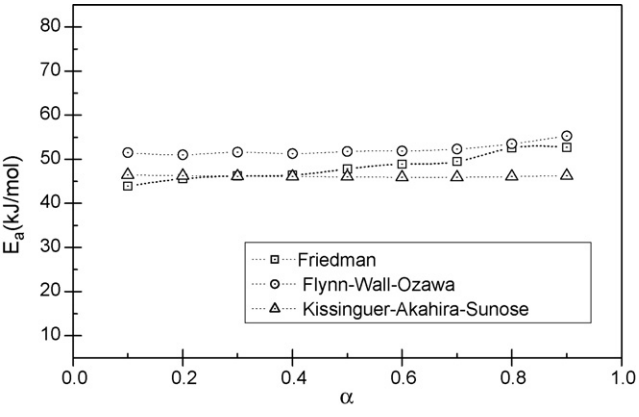

Fig. 12. Activation energies as function of conversion obtained by different dynamic methods.

where T_α is the temperature at which a conversion α is reached in the non-isothermal run, T_0 the temperature at which the curve $\alpha(t)$ has to be computed, and t_α is the time required for reaching a conversion α at a temperature T_0. Solving the right-hand side integral of Eq. (20) using the afore-mentioned Coats–Redfern approach leads to:

$$t_\alpha = \frac{RT_\alpha^2}{\beta E_{a\alpha}} \exp\left[\frac{E_{a\alpha}}{R}\left(\frac{1}{T_0} - \frac{1}{T_\alpha}\right)\right] \quad (21)$$

Knowing the pairs E_α, T_α, the time, t_α, at which those conversions would be reached at a temperature T_0 can be now calculated.

Using the Friedman $E(\alpha)$ dependence a set of t_α values for different conversions and different temperatures were computed. Friedman method resulted to give better fit than the other two methods and only its prediction is shown in Fig. 13. Fig. 13 compares the predicted isotherms with those experimentally obtained. The deviation at intermediate conversions was matched to the high heating rates used for the non-isothermal measurements, deviating from the isothermal behaviour of the reaction. Thus, it is inferred that slower heating rates would lead to more adjusted $\alpha(t)$ curves. Another important reason that explains this deviation is the differences between isothermal and dynamically obtained $E(\alpha)$ dependencies. Other reason for the observed deviation could be, as appointed by Criado et al. [51], the arising for considering the preexponential or frequency factor independent of temperature, when calculating $E(\alpha)$.

4.3. Thermodynamics

To understand the autocatalytic mechanism of the urethane reaction a thermodynamic analysis is useful. Although till now a non-temperature dependent pre-exponential factor has been considered for calculating the values of the kinetic constants in the iteration of Eq. (5) a qualitative study in which kinetic constants with temperature dependent pre-exponential factors are assumed can be made for the calculation of thermodynamic activations parameters.

Wynne-Jones–Eyring–Evans theory [49,52] presents a temperature dependent preexponential factor, with which the kinetic

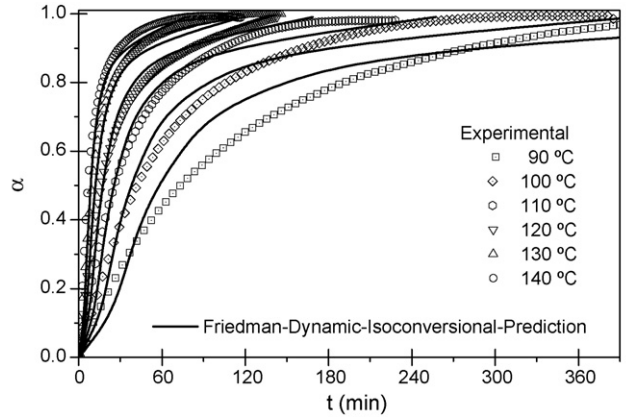

Fig. 13. Conversion vs. time isotherms predicted by non-isothermal data at temperatures T_0, from 90 to 140 °C.

Table 2
Activation parameters calculated according to Wynne-Jones–Eyring–Evans equations, for non-catalyzed and catalyzed polydiol/HDI system reaction paths

Reaction path	$\Delta H^{\#}$ (kJ/mol)	$\Delta S^{\#}$ (J K^{-1} mol^{-1})
Non-catalyzed	40.2	−173.5
Autocatalyzed	86.7	−52.1

constant becomes:

$$k = \frac{k_B T^n}{h} \exp\left[N + \frac{\Delta S^{\#}}{R}\right] \exp\left[\frac{-E_a}{RT}\right] \quad (22)$$

where k_B and h are the Boltzmann and Planck constants, respectively, N the so-called molecularity, $\Delta S^{\#}$ is the activation entropy and $E_a = \Delta H^{\#} + NRT$, a function of activation enthalpy, $\Delta H^{\#}$, and molecularity. The classical Arrhenius constants have $N = 0$. N uses to be 1 for reactions occurring in liquid state [49]. Thus, assuming $N = 1$, plotting $\ln(k/T)$ against $1/T$, $\Delta H^{\#}$ and $\Delta S^{\#}$ are obtained from the slope and origin, respectively.

Table 2 presents values for activation enthalpies, $\Delta H^{\#}$, and entropies, $\Delta S^{\#}$, calculated using the absolute kinetic constants obtained from the iteration of Eq. (5) for the HDI system studied in this work. Thus, activation enthalpy and entropy pairs for both non-catalyzed reaction path, $\Delta H_1^{\#}$ and $\Delta S_1^{\#}$, and autocatalyzed reaction path, $\Delta H_2^{\#}$ and $\Delta S_2^{\#}$, were obtained. For results analysis, it is interesting to bear on mind the definition of entropy variation, $\Delta S = S_{final} - S_{initial}$. Considering a similar entropic initial state for both non-catalyzed and urethane catalyzed reactions (i.e. when molecules are very separated one to each other), a lower value for the entropy of non-catalyzed activation state, $\Delta S_1^{\#}$, than that for the autocatalyzed, $\Delta S_2^{\#}$, would suggest a final state of the non-catalyzed reaction path more ordered, what is thermodynamically disfavoured. This fact makes this reaction path more and more disfavoured while the temperature increases, and that could be the reason that explains the more noticeable autocatalytic effect at high temperatures.

Negative values for activation entropies also indicate the importance of reactants association previous to chemical reaction [49,53], thus reinforcing the certainty of an autocatalytic mechanism for polyurethanes systems.

The higher activation energy values obtained for the aliphatic studied system than for the aromatic ones found in the literature can be explained taking into account thermodynamic aspects. In this way some authors [30,44] have appointed that due to the more stable activated complex of aromatic diisocyanate compounds, owed to the conjugation of double bonds between the aromatic ring and NCO group, these aromatic diisocyanates present a higher tendency to associate therefore giving higher kinetic constants.

5. Conclusions

Free external catalysis cure kinetics of a new biodegradable polyurethane system formed by poly(hexamethylene carbonate-*co*-caprolactone)diol and aliphatic hexamethylene diisocyanate has been characterized by DSC, FT-IR and ^{13}C NMR. The polymerization process is rather slow at temperatures below 80 °C and much slower than that for other polyurethane systems such as those containing aromatic diisocyanates, what can be explained taking into account thermodynamics aspects. Even high temperatures were employed in the polymerizations no significant lateral reactions were observed within the range 80–140 °C by ^{13}C NMR and FT-IR.

Although Sato's autocatalytic equation has been previously used to describe aliphatic and aromatic diisocyanates autocatalytic systems, that model was not able to describe the present autocatalytic polyurethane cure.

Both kinetic modelling and model-free methods have been successfully applied for describing the cure of the polyurethane autocatalytic system. These models are able to predict the kinetic behaviour at different temperatures.

No lateral reaction were observed by ^{13}C NMR, which together with the thermodynamic consideration, suggests that autocatalysis, is undergone by urethane group via an urethane–alcohol intermediate, this effect being more noticeable at elevated temperatures.

Acknowledgments

The authors wish to express their gratitude to Gipuzkoako Foru Aldundia-Diputación Foral de Gipuzkoa (0207/2005) and also to Basque Government '*Etortek 2005*/*BiomaGUNE 2005*' (IE05-143) for financial support. The authors are also grateful to L. Irusta, from the Faculty of Chemistry of Donostia-San Sebastian, for NMR analyses. P.M. Stefani wishes to express his gratitude to CONICET for their financial support.

References

[1] S. Gogolewsky, Colloid Polym. Sci. 267 (1989) 757.
[2] K. Gorna, S. Gogolewsky, J. Biomed. Mater. Res. 67A (2003) 813.
[3] K. Gorna, S. Polowinsky, S. Gogolewsky, J. Polym. Sci., Part A: Polym. Chem. 40 (2002) 156.
[4] Y.W. Tang, R.S. Labow, J.P. Santerre, J. Biomed. Mater. Res. 57 (2001) 597.
[5] R.S. Labow, E. Meek, J.P. Santerre, Biomaterials 22 (2001) 3025.
[6] Y.W. Tang, R.S. Labow, J.P. Santerre, Biomaterials 24 (2003) 2805.
[7] N. Sbirrazzuoli, S. Vyazovkin, Thermochim. Acta 388 (2002) 289.
[8] S. Vyazovkin, N. Sbirrazzuoli, Macromolecules 29 (1996) 1867.
[9] N. Sbirrazzuoli, S. Vyazovkin, A. Mititelu, C. Sladic, L. Vicent, Macromol. Chem. Phys. 204 (2003) 1815.
[10] R.B. Prime, Polym. Eng. Sci. 13 (1973) 365.
[11] F. Chu, T. McKenna, S. Lu, Eur. Polym. J. 33 (1997) 837.
[12] K. Pielichowski, P. Czub, J. Pielichowski, Polymer 41 (2000) 4381.
[13] J. Macan, I. Brnardic, M. Ivankovic, H.J. Mencer, J. Therm. Anal. Cal. 81 (2005) 369.
[14] J.M.E. Rodrigues, M.R. Pereira, A.G. de Souza, M.L. Carvalho, A.A. Dantas Neto, T.N.C. Dantas, J.L.C. Fonseca, Thermochim. Acta 427 (2005) 31.
[15] F. Dimier, N. Sbirrazzuoli, B. Vergnes, M. Vincent, Polym. Eng. Sci. 44 (2004) 518.
[16] W. Sultan, J.P. Busnel, J. Therm. Anal. Cal. 2 (2006) 355.
[17] S. Li, E. Vuorimaa, H. Lemmetyinen, J. Appl. Polym. Sci. 81 (2001) 1474.
[18] S. Li, R. Vatanparast, E. Vuorimaa, H. Lemmetyinen, J. Polym. Sci., Part B: Polym. Phys. 38 (2000) 2213.
[19] P.M. Stefani, S.M. Moschiar, M.I. Aranguren, J. Appl. Polym. Sci. 73 (2001) 1771.
[20] H.E. Kissinger, Anal. Chem. 29 (1957) 1702.

[21] M.R. Kamal, S. Sourour, Polym. Eng. Sci. 13 (1973) 59.
[22] J.L. Martin, A. Cadenato, J.M. Salla, Thermochim. Acta 306 (1997) 115.
[23] J.M. Salla, A. Cadenato, X. Ramis, J.M. Morancho, J. Therm. Anal. Cal. 56 (1999) 771.
[24] M. Daviti, K. Chrissafis, K.M. Paraskevopoulos, E.K. Polychroniadis, T. Spassov, J. Therm. Anal. Cal. 70 (2002) 605.
[25] C. Jubsilp, S. Damrongsakkul, T. Taeichi, S. Rimdusit, Thermochim. Acta 44 (2006) 131.
[26] S. Li, P. Järvelä, J. Polym. Sci., Part B: Polym. Phys. 39 (2001) 1525.
[27] L. Núñez, F. Fraga, A. Castro, M.R. Núñez, M. Villanueva, J. Appl. Polym. Sci. 77 (2000) 2285.
[28] E.G. Prout, E.C. Tompkins, Trans. Faraday Soc. 40 (1944) 488.
[29] J.M. Kenny, J. Appl. Polym. Sci. 51 (1994) 761.
[30] J. Sato, J. Org. Chem. 82 (1960) 3893.
[31] A. Eceiza, J. Zabala, J.L. Egiburu, M.A. Corcuera, I. Mondragon, J.P. Pascault, Eur. Polym. J. 35 (1999) 1949.
[32] P. Simon, J. Therm. Anal. Cal. 76 (2004) 123.
[33] S. Vyazovkin, N. Sbirrazzuoli, Macromol. Rapid Commun. 27 (2006) 1515.
[34] P. Budrugeac, D. Homentcovschi, E. Segal, J. Therm. Anal. Cal. 63 (2001) 457.
[35] S. Vyazovkin, J. Comp. Chem. 22 (2001) 178.
[36] H.L. Friedman, J. Polym. Sci., Part C 6 (1965) 183.
[37] J.H. Flynn, L.A. Wall, J. Res. Natl. Bur. Stan. A: Phys. Chem. 70A (1966) 487.
[38] T. Ozawa, Bull. Chem. Soc. Jpn. 38 (1965) 1881.
[39] C. Doyle, J. Appl. Polym. Sci. 6 (1962) 639.
[40] A.W. Coats, J.P. Redfern, Nature 201 (1964) 68.
[41] P. Chaffanjon, R.A. Grisby Jr., E.L. Rister Jr., R.L. Zimmerman, J. Cell Plast. 39 (2003) 187.
[42] A. Eceiza, K. de la Caba, V. Gascon, M.A. Corcuera, I. Mondragon, Eur. Polym. J. 37 (2001) 1685.
[43] A. Eceiza, K. de la Caba, G. Kortaberria, N. Gabilondo, C. Marieta, M.A. Corcuera, I. Mondragon, Eur. Polym. J. 41 (2005) 3051.
[44] L. Thiele, R. Becker, Adv. Urethane Sci. Technol. 3 (1993) 59.
[45] M.E. Ghafari, Q.T. Pham, Makromol. Chem. 184 (1983) 1669.
[46] J.F. Gerard, Makromol. Chem. 189 (1988) 1693.
[47] C. Pavier, A. Gandini, Eur. Polym. J. 36 (2000) 1653.
[48] A.V. Cunliffe, A. Davis, M. Farey, J. Writh, Polymer 26 (1985) 301.
[49] H.E. Avery, Basic reaction kinetics and mechanisms, in: Theory of Reaction Rates, Macmillan, London, 1974, p. 69.
[50] S.V. Vyazovkin, A.I. Lesnikovich, Thermochim. Acta 203 (1992) 177.
[51] M. Criado, L.A. Pérez-Maqueda, P.E. Sánchez-Jiménez, J. Therm. Anal. Cal. 82 (2005) 671.
[52] W.F.K. Wynne-Jones, H. Eyring, J. Chem. Phys. 3 (1935) 492.
[53] D. Kincal, S. Özkar, J. Appl. Polym. Sci. 66 (1997) 1979.